EFFECT OF ANISOTROPIC YIELD CRITERION ON THE SPRINGBACK IN PLANE STRAIN PURE BENDING

F.V. Grechnikov[1,2], Ya.A. Erisov[1], S.E. Alexandrov[3]

[1]Samara National Research University, Samara, Russia
[2]Samara Scientific Center of Russian Academy of Sciences, Samara, Russia
[3]Institute for Problems in Mechanics, Russian Academy of Sciences, Moscow, Russia

Abstract. Plastic anisotropy is one of the multiple material representations significantly affecting the springback simulations. The present paper studies the influence of the plastic anisotropy over the springback in plane strain pure bending by means of the exact semi-analytical solution. The yield criterion and the constitutive equations for the orthotropic material with consideration of the crystal lattice constants and parameters of the crystallographic texture are used taking into account the anisotropy.

Keywords: anisotropy, crystallographic orientation, yield criterion, springback, bending, plane strain, elastic/plastic solution.

Citation: Grechnikov FV, Erisov YaA, Alexandrov SE. Effect of anisotropic yield criterion on the Springback in plane strain pure bending. CEUR Workshop Proceedings, 2016; 1638: 569-577. DOI: 10.18287/1613-0073-2016-1638-569-577

1 Introduction

As it is evident from the production analysis of the Russian plants the metal loss in sheet metal forming processes only amounts up to 45-50%: metal utilization factor in aircraft industry is about 40%, in engine industry - 30% and in automotive industry - 50%. Presumably, waste is much higher due to the collateral loss (about 10-15%). In a greater degree, these losses arise from the undesirable anisotropy of the blank properties.
For most materials the anisotropy of physical and mechanical properties is a rule rather than an exception [1]. Generally, anisotropy, which stems from the crystal structure of materials, determines processing and service characteristics of the products. As to metal forming processes, the undesirable anisotropy not only distorts the shapes and sizes of the parts, but also limits the formability, causing the excessive thinning of the material [2]. Therefore, in order to compensate thinning, it is necessary to increase the initial sizes of the blanks, which in turn results in the metal loss, the weight

growth of the construction, the technological cycle extension, and, consequently, in the numerous additional expenses (equipment, areas, power resources, workers, etc).
However, as it follows from the numerous researches [3-6], the influence of anisotropy has more advantages rather than disadvantages. For example, the considerable achievements in material science of the electric steels (e.g. increasing magnetic induction and capacitance, cutting electric power losses) became possible mainly due to developing efficient anisotropy of physical properties [7-8].
From the above it appears, firstly, the instant necessity of the anisotropy impact assessing in processing and service characteristics of products; secondly, the necessity of developing special methods for obtaining and efficient application of anisotropy. Unfortunately, the imperfection of the process design techniques does not allow considering anisotropy of the blank properties [9-10] and, as a result, makes the excessive metal consumption inevitable at the production stage.
A comprehensive overview on springback that follows a sheet forming process when the forming loads are removed from the workpiece has been provided in [11]. It is emphasized that plastic anisotropy is one of the various material representations that significantly affects the springback simulations. In the present paper, the effect of the springback plastic anisotropy in the plane strain pure bending is studied by means of the exact semi-analytical solution.

2 Theory of bending at large strain

The theory of the elastic/plastic plane strain bending of an incompressible anisotropic sheet obeying the quadratic Hill yield criterion [12] has been presented in the article [13]. Ultimately, the main results of this work are represented in this section. The solution is based on the following mapping between the Eulerian Cartesian coordinate system (x, y) and the Lagrangian coordinate system (ζ, η)

$$\frac{x}{H}=\sqrt{\frac{\zeta}{a}+\frac{s}{a^2}}\cos(2a\eta)-\frac{\sqrt{s}}{a},\qquad \frac{y}{H}=\sqrt{\frac{\zeta}{a}+\frac{s}{a^2}}\sin(2a\eta), \tag{1}$$

where H is the initial thickness of the sheet, s is an arbitrary function of a, which is a function of the time, t, and $a=0$ at $t=0$. It follows from Eq. (1) that $x=\zeta H$ and $y=\eta H$ at $a=0$ if

$$s=1/4 \text{ at } a=0. \tag{2}$$

It can be verified by the inspection through the application of l'Hospital's rule to Eq. (1), with the use of Eq. (2), as $a\to 0$. Eq. (1) and (2) a transformation description of the rectangle defined at the initial instant $a=0$, by the equations $x=-H$, $x=0$ and $y=\pm L$ (or, in the Lagrangian coordinates, by the equations $\zeta=-1$, $\zeta=0$ and $\eta=\pm L/H$) into the shape determined by the two circular arcs, *AD* and *CB*, and the two straight lines, *AD* and *CB* (Fig. 1).
It is convenient to introduce a moving cylindrical coordinate system (r, θ) by the equations of transformation

$$\frac{x}{H}+\frac{\sqrt{s}}{a}=\frac{r\cos\theta}{H} \text{ and } \frac{y}{H}=\frac{r\sin\theta}{H}. \tag{3}$$

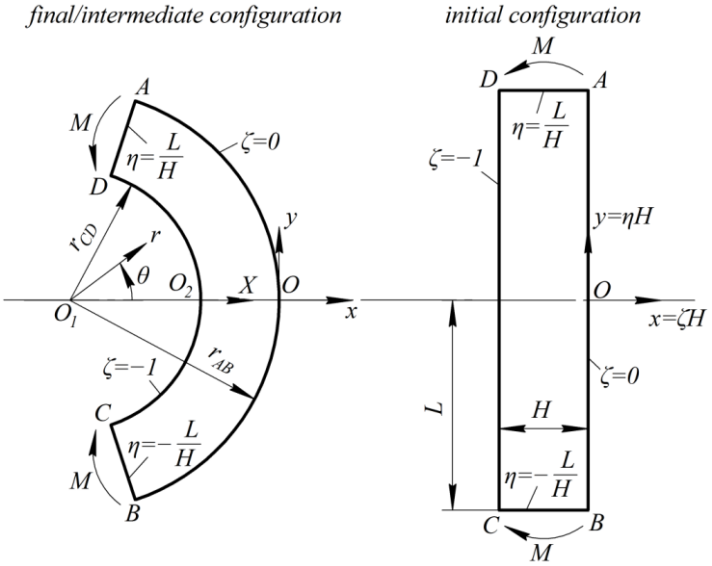

Fig. 1. Geometry of the process - notation

The origin of this coordinate system is located at $x/H=-\sqrt{s}/a$ and $y=0$. The lines *CB* and *DA* are determined by the equations $\theta=\pm\theta_0$, and the lines *AB* and *CD* by the equations $r=r_{AB}$ and $r=r_{CD}$, respectively (Fig. 1). θ_0, r_{AB}, and r_{CD} are the functions of a. Using Eq. (1), it is also possible to get the following relations

$$\frac{r_{AB}}{H}=\frac{\sqrt{s}}{a},\quad \frac{r_{CD}}{H}=\sqrt{\frac{s}{a^2}-\frac{1}{a}},\quad \theta_0=\frac{2aL}{H},\ \frac{h}{H}=\frac{\sqrt{s}-\sqrt{s-a}}{a}, \tag{4}$$

where h is the current thickness.

In the case of the elastic/plastic bending, there are two plastic regions and one elastic region. Let $\zeta=\zeta_1(a)$ and $\zeta=\zeta_2(a)$ be the elastic-plastic boundaries moving from $\zeta=0$ and $\zeta=-1$, respectively. Then, the distribution of the stresses is given by

$$\frac{\sigma_{\zeta\zeta}}{T}=\ln\left(\frac{\zeta a+s}{s}\right),\ \frac{\sigma_{\eta\eta}}{T}=\ln\left(\frac{\zeta a+s}{s}\right)+2 \tag{5}$$

in the region $\zeta_1(a)\le\zeta\le 0$,

$$\frac{\sigma_{\zeta\zeta}}{T}=-\ln\left(\frac{\zeta a+s}{s-a}\right),\ \frac{\sigma_{\eta\eta}}{T}=\ln\left(\frac{s-a}{\zeta a+s}\right)-2 \tag{6}$$

in the region $-1\le\zeta\le\zeta_2(a)$ and

$$\frac{\sigma_{\zeta\zeta}}{T}=\frac{1}{p}\ln^2\left[4\left(\zeta a+s\right)\right]+\frac{p}{4}-\ln\left(4s\right),$$
$$\frac{\sigma_{\eta\eta}}{T}=\frac{1}{p}\ln^2\left[4\left(\zeta a+s\right)\right]+\frac{p}{4}-\ln\left(4s\right)+\frac{4}{p}\ln\left[4\left(\zeta a+s\right)\right] \quad (7)$$

in the region $\zeta_2(a)\le\zeta\le\zeta_1(a)$. Here

$$s=\frac{2a+\sqrt{1+4a^2}}{4},\ \zeta_1(a)=\frac{\exp(p/2)-4s}{4a},\ \zeta_2(a)=\frac{\exp(-p/2)-4s}{4a},$$
$$T=\frac{X^2Y^2Z}{\sqrt{2X^2Y^2Z^2\left(Y^2+Z^2\right)-Y^4Z^4-X^4\left(Y^2-Z^2\right)^2}},\ p=\frac{2T}{G}, \quad (8)$$

where X, Y and Z are the tensile yield stresses in the ζ -, η - and z - directions, respectively, and G is the shear modulus of elasticity.

The bending moment per unit length is defined by

$$M=\int_{r_{CD}}^{r_{AB}}\sigma_{\eta\eta}r\mathrm{d}r.$$

Using Eq. (1) and (3), this equation can be transformed to

$$m=\frac{2M}{TH^2}=\frac{1}{a}\int_{-1}^{0}\frac{\sigma_{\eta\eta}}{T}\mathrm{d}\zeta, \quad (9)$$

where m is the dimensionless bending moment.

In the case of the purely elastic unloading, the stress increments are

$$\frac{\Delta\sigma_{\zeta\zeta}}{T}=\frac{4}{p}C_1\left[\frac{\left(R_0^2-R_1^2\right)}{R_1^2\ln\left(R_1/R_0\right)}\ln\left(\frac{r}{R_0}\right)-\left(\frac{R_0}{r}\right)^2+1\right],$$
$$\frac{\Delta\sigma_{\eta\eta}}{T}=\frac{4}{p}C_1\left\{\frac{\left(R_0^2-R_1^2\right)}{R_1^2\ln\left(R_1/R_0\right)}\left[\ln\left(\frac{r}{R_0}\right)+1\right]+\frac{R_0^2}{r^2}+1\right\}, \quad (10)$$
$$C_1=\frac{m_f p}{2}\left(\frac{H}{R_0}\right)^2\left[\frac{\left(R_1^2/R_0^2-1\right)^2}{\left(R_1^2/R_0^2\right)\ln\left(R_1/R_0\right)}-4\ln\left(\frac{R_1}{R_0}\right)\right]^{-1}.$$

Here m_f, R_0 and R_1 are the values of m, r_{CD} and r_{AB} at the end of loading. Also,

$$\frac{r}{H}=\sqrt{\frac{\zeta}{a_f}+\frac{s_f}{a_f^2}}, \quad (11)$$

where a_f and s_f are the values of a and s at the end of loading. Using Eq. (7), in which a and s should be replaced with a_f and s_f from Eq. (11), the variation of

$\sigma_{\zeta\zeta}$ and $\sigma_{\eta\eta}$ with r/H at the end of loading is determined in parametric form with ζ being the parameter. Then, the distribution of the residual stresses are found from $\sigma_{\zeta\zeta}^{res} = \sigma_{\zeta\zeta}^{f} + \Delta\sigma_{\zeta\zeta}$, $\sigma_{\eta\eta}^{res} = \sigma_{\eta\eta}^{f} + \Delta\sigma_{\eta\eta}$.

The radius r_{CD} after unloading, R_u, is determined as

$$\frac{R_u}{R_0} = 1 + C_1 - \frac{C_1\left(R_0^2 - R_1^2\right)}{2R_1^2 \ln\left(R_1/R_0\right)}. \tag{12}$$

3 Material model

Let us consider the bending of orthotropic rolled sheet. The principal axes of orthotropy coincide with the coordinate lines of the Cartesian coordinate system: *x*, *y* and *z* are thickness, transverse and rolling directions, respectively, i.e. in the case under consideration the bending line coincides with rolling direction. Therefore, the yield function proposed in [14] is:

$$\begin{aligned}&\eta_{23}\left(\sigma_{xx} - \sigma_{yy}\right)^2 + \eta_{12}\left(\sigma_{yy} - \sigma_{zz}\right)^2 + \eta_{31}\left(\sigma_{zz} - \sigma_{xx}\right)^2 + \\ &+4\left[\left(\frac{5}{2} - \eta_{23}\right)\sigma_{xy}^2 + \left(\frac{5}{2} - \eta_{12}\right)\sigma_{yz}^2 + \left(\frac{5}{2} - \eta_{31}\right)\sigma_{zx}^2\right] = 2\sigma_{eq}^2.\end{aligned} \tag{13}$$

Here σ_{eq} is the equivalent stress, σ_{ij} are the components of the stress tensor in the Cartesian system of coordinates. The generalized anisotropy factors η_{ij} are defined as

$$\eta_{ij} = 1 - \frac{15\left(A' - 1\right)}{3 + 2A'}\left(\Delta_i + \Delta_j - \Delta_k - \frac{1}{5}\right), \tag{14}$$

where A' is the anisotropy factor of a crystal lattice, Δ_i are the parameters of the crystallographic texture. The anisotropy factor is defined through the compliance constants of crystal lattice S'_{1111}, S'_{1122} and S'_{2323}

$$A' = \frac{S'_{1111} - S'_{1122}}{2S'_{2323}}. \tag{15}$$

For a certain crystallographic orientation $\{hkl\}\langle uvw\rangle$ the parameters of the crystallographic texture are defined as

$$\Delta_i = \frac{h_i^2 k_i^2 + k_i^2 l_i^2 + l_i^2 h_i^2}{\left(h_i^2 + k_i^2 + l_i^2\right)^2}, \tag{16}$$

where h_i, k_i, l_i are Miller's indices, which determine the *i*-th direction in the crystal with respect to the principal axes of anisotropy.

Considering the tension along the principal axes, let us determine the tensile yield stresses from Eq. (13):

$$X = \sqrt{\frac{\eta_{12}+\eta_{23}}{\eta_{23}+\eta_{31}}}Y = \sqrt{\frac{\eta_{12}+\eta_{31}}{\eta_{23}+\eta_{31}}}Z\,. \tag{17}$$

Using Eq. (17), the last equation of (8) can be transformed into

$$p = \frac{Z}{G}\frac{\eta_{12}+\eta_{31}}{\sqrt{\eta_{12}\eta_{23}+\eta_{23}\eta_{31}+\eta_{31}\eta_{12}}}\,, \tag{18}$$

where Z is the tensile yield stress in the rolling direction.

Thus, the material model considers the crystal lattice constants (A'), i.e. chemical composition of alloy, and the crystallographic texture (Δ_i), i.e. its thermo-mechanical treatment. Using this model, it is possible to analyze the influence of the ideal crystallographic orientations over the springback in bending.

4 Numerical results

Let us consider the copper sheet for which components of compliance tensor are $S'_{1111} = 15.0$ TPa^{-1}; $S'_{1122} = -6.30$ TPa^{-1} and $S'_{2323} = 3.33$ TPa^{-1} [15], i.e. $A' = 3.203$ (Eq. (15)); the tensile yield stress in the rolling direction Z is 340 MPa; the shear modulus of elasticity G is 44 GPa. As an example, let us take the following ideal crystallographic orientations: copper {112}<111>, brass {110}<112> (rolling components) and Goss {110}<001> (recrystallization component). Also, as a comparison let us consider the isotropic case, for which $A' = 1$ or $\Delta_i = 1/5$ [16], i.e. $\eta_{ij} = 1$.

The parameters of crystallographic texture Δ_i, generalized anisotropy factors factors η_{ij} and parameter p calculated using Eq. (16), (14) and (18) for the stated components are listed in Table 1.

Table 1. The parameters of crystallographic texture and the generalized anisotropy factors of the single ideal components

Component		**The parameters of crystallographic texture**			**The generalized anisotropy factors**			$p \cdot 10^{-3}$
Name	Orientation	Δ_1	Δ_2	Δ_3	η_{12}	η_{23}	η_{31}	
Copper	{112}<111>	0.333	0.250	0.250	0.533	1.116	0.533	6.785
Brass	{110}<112>	0.250	0.333	0.250	0.533	0.533	1.116	10.496
Goss	{110}<001>	0.0	0.250	0.250	1.703	-0.054	1.703	15.969
Isotropy	-	0.200	0.200	0.200	1.0	1.0	1.0	8.923

The dependence of the bending moment on the radius of the concave surface at the beginning of the process is shown in Fig. 2. It is seen from this diagram that the effect of anisotropy is revealed at the very beginning of the process only. Note that the required bending moment for some ideal crystallographic orientations can be bigger ({112}<111>) or smaller ({110}<112>, {110}<001>) in comparison with the isotropic material.

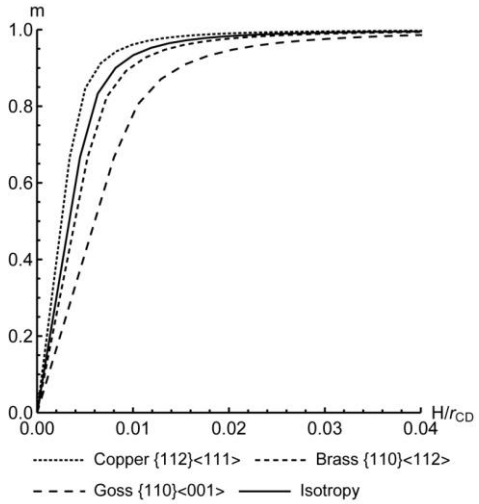

Fig. 2. Effect of ideal crystallographic orientations on the bending moment

The dependence of the springback R_u/R_0 on value of radius r_{CD} is depicted in Fig. 3. The figure shows that the springback decreases as the deformation at the end of loading increases. All other things being equal the orientations {110}<112> and {110}<001> cause bigger springback than the isotropic material and orientation {112}<111>, for which the springback is minimal.

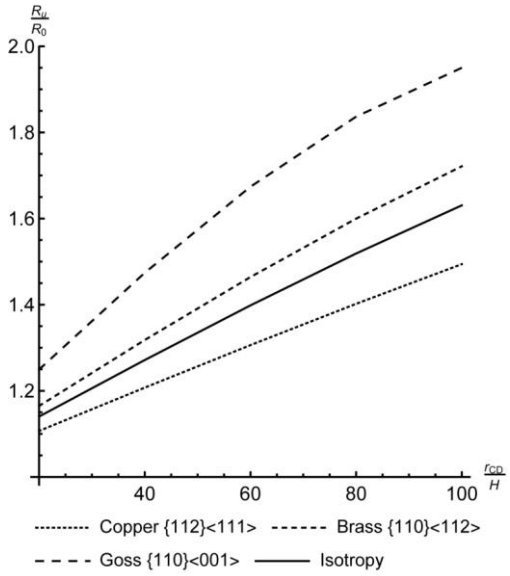

Fig. 3. Dependence of the springback on the radius at the end of loading

The influence of the ideal crystallographic orientations upon the thickness distribution of the residual stresses is illustrated in Fig. 4. In particular, the radial stress is shown in Fig. 4a and the circumferential stress in Fig. 4b at $r_{CD}/H = 60$. The figures specified reveal that the effect of anisotropy is most significant at the central part of the specimen. The distribution of the residual stresses outside the central part of the specimen is almost independent from the crystallographic orientation except for {110}<001>.

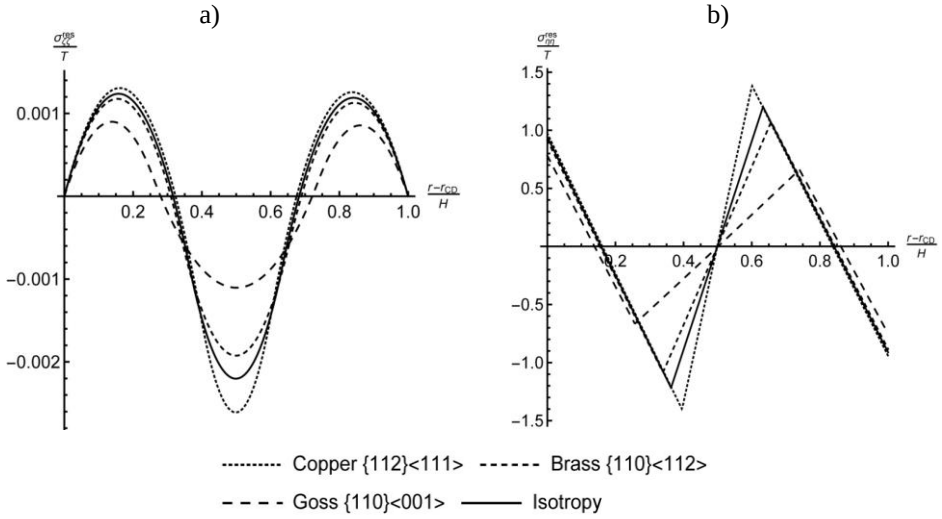

Fig. 4. Through thickness distribution of the radial (a) and circumferential (b) residual stresses at $r_{CD}/H = 60$ at the end of loading

5 Conclusions

The plane strain pure bending of materials textured has been investigated. It has been stated that depending on the ideal crystallographic orientations the springback and the distribution of the residual stresses change grossly. Note that the springback of the textured metal sheet can be bigger ({110}<112>, {110}<001>) or smaller ({112}<111>) in comparison with the isotropic material.

Acknowledgements

The reported study was funded by RFBR according to the research project №16-38-00495.

References

1. Backofen WA. Deformation Processing. Metall. Trans., 1973; 4: 2679-2699.
2. Banabic D, Barlat F, Cazacu O, Kuwabara T. Advances in anisotropy and formability. International Journal of Material Forming, 2010; 3: 165-189.
3. Engler O, Hirsch J. Texture control by thermomechanical processing of AA6xxx Al-Mg-Si sheet alloys for automotive applications - a review. Materials Science and Engineering A, 2002; 336: 249-262.
4. Tóth LS, Hirsch J., Van Houtte P. On the role of texture development in the forming limits of sheet metals. International Journal of Mechanical Sciences, 1996; 38: 1117-1126.
5. Hutchinson WB, Oscarsson A, Karlsson A. Control of microstructure and earing behaviour in aluminium alloy AA 3004 hot bands. Materials Science and Technology, 1989; 5: 1118-1127.
6. Andrianov AV, Kandalova EG, Aryshensky EV, Grechnikova AF. Influence of 3104 Alloy microstructure on sheet performance in ironing aluminum beverage cans. Key Engineering Materials, 2016; 684: 398-405.
7. Moses AJ. Electrical steels. Past, present and future developments. IEE Proceedings A: Physical Science. Measurement and Instrumentation. Management and Education. Reviews, 1990; 137: 233-245.
8. Shirkoohi GH, Arikat MAM. Anisotropic properties of high permeability grain-oriented 3.25% Si-Fe electrical steel. IEEE Transactions on Magnetics, 1994; 30: 928-930.
9. Campbell FC. Manufacturing Technology for Aerospace Structural Materials. Oxford: Elsevier, 2006; 600 p.
10. Guo ZX. The Deformation and Processing of Structural Materials. Cambridge: Woodhead Publishing, 2005; 331 p.
11. Wagoner RH, Lim H, Lee M-G. Advances issues in springback. International Journal of Plasticity, 2013; 45: 3-20.
12. Hill R. The Mathematical Theory of Plasticity. Oxford: Clarendon Press, 1950; 366 p.
13. Alexandrov S, Hwang Y-M. The Bending Moment and Springback in Pure Bending of Anisotropic Sheets. Int. J. Solids Struct., 2009; 46(25-26): 4361-4368.
14. Erisov YA, Grechnikov FV, Surudin SV. Yield function of the orthotropic material considering the crystallographic texture. Structural Engineering and Mechanics, 2016; 58(4): 7-18.
15. Landolt-Bornstein. Numerical data and functional relationships in science and technology. New Series. Group III: Crystal and solid state physics. Volume 1: Elastic, piezoelectric, piezooptic and electrooptic constants of crystals. Berlin: Springer, 1966; 643 p.
16. Adamesku PA, Geld RA, Mityshov EA. Anisotropy of Physical Properties of Metals. Moscow: Mashinostroenie, 1985; 136 p. [in Russian]